Available online at www.sciencedirect.com
ScienceDirect
Journal of Power Sources 167 (2007) 64–68
JOURNAL OF POWER SOURCES
www.elsevier.com/locate/jpowsour

Short communication

Preparation and electrochemical properties of a $Sm_{2-x}Sr_xNiO_4$ cathode for an IT-SOFC

Qiang Li [a], Yong Fan [a], Hui Zhao [b,*], Li-Ping Sun [b], Li-Hua Huo [b]

[a] *College of Material Science and Engineering, Harbin University of Science and Technology, Harbin 150080, PR China*
[b] *School of Chemistry and Materials Science, Heilongjiang University, Harbin 150080, PR China*

Received 20 December 2006; received in revised form 7 February 2007; accepted 8 February 2007
Available online 21 February 2007

Abstract

Cathodic materials $Sm_{2-x}Sr_xNiO_4$ ($0.5 \leq x \leq 1.0$) for an IT-SOFC (intermediate temperature solid oxide fuel cell) were prepared by the glycine-nitrate process and characterized by XRD, SEM, ac impedance spectroscopy and dc polarization measurements. The results showed that no reaction occurred between the $Sm_{2-x}Sr_xNiO_4$ electrode and the $Ce_{0.9}Gd_{0.1}O_{1.9}$ (CGO) electrolyte at 1100 °C, and the electrode formed good contact with the electrolyte after sintering at 1000 °C for 2 h. The electrochemical properties of these cathode materials were studied using impedance spectroscopy at various temperatures and oxygen partial pressures. $Sm_{1.0}Sr_{1.0}NiO_4$ exhibited the lowest cathodic overpotential. The area specific resistance (ASR) was 3.06 Ω cm^2 at 700 °C in air.
© 2007 Elsevier B.V. All rights reserved.

Keywords: Intermediate temperature solid oxide fuel cell (IT-SOFC); SSN cathode material; Electrode reaction

1. Introduction

Solid oxide fuel cells (SOFCs) are electrochemical devices that convert the chemical energy of a fuel into electrical energy in a clean, cheap, and efficient way [1]. There is increasing interest in the development of intermediate temperature solid oxide fuel cells (IT-SOFCs). Reduced operation temperature can reduce problems with sealing and thermal degradation, and allows the use of low-cost interconnection materials. Although improvement has been made, reducing the operation temperature to 500–800 °C without a significant decrease of the power density remains the challenge for this technology [2,3].

Nickelates with a K_2NiF_4-type structure have been investigated previously with respect to their superconducting properties at low temperatures [4]. Recently, these oxides were extensively re-examined concerning their possible usage as cathode materials of IT-SOFC. Studies showed that these materials exhibited mixed ionic electronic conducting properties, substantial oxygen permeability and a relatively low thermal and chemical induced expansion coefficient [5,6]. Some preliminary studies of these materials in terms of oxygen diffusion and surface exchange coefficients have been reported [7]. Research has also proved that at higher temperatures and lower oxygen partial pressures, the K_2NiF_4-type oxides have a higher thermochemical stability compared with the ABO_3-type oxides [6]. This implies that K_2NiF_4-type oxides are likely to be suitable cathode materials of IT-SOFC.

At present, most of the research has been concentrated on La_2NiO_4 based materials, with either replacing lanthanum with other rare earth elements, and/or doping wirh some transitional metals [8,9]. Few papers consider the effect of doping in the A site of the A_2BO_4-type nickelate for changing cathodic properties. It was reported that Sr-doping improved the p-type electrical conductivity of $La_{2-x}Sr_xNiO_4$ nickelates [10], and different kinds of oxygen defects could be formed, depending on the Sr-doping concentration, the oxygen partial pressure and the preparation temperature [5,11]. It was generally believed that these oxygen defects offered the possibility of rapid oxygen transport through the ceramic material. We have found in our previous study that Sr-doping in $La_{2-x}Sr_xNiO_4$ could improve its cathodic properties [12]. The similar result was found in Sr doped $A_{2-\alpha}A'_\alpha MO_4$ (A = Pr, Sm; A′ = Sr; B = Fe, Co) [13]. Compared to $La_{2-x}Sr_xNiO_4$ material, $Sm_{2-x}Sr_xNiO_4$ has lower thermal expansion coefficient and higher conductivity

* Corresponding author. Tel.: +86 45186608040; fax: +86 45186608040.
E-mail address: zhaohui98@yahoo.com (H. Zhao).

0378-7753/$ – see front matter © 2007 Elsevier B.V. All rights reserved.
doi:10.1016/j.jpowsour.2007.02.018

[14], which fulfills the basic requirement of cathode materials for IT-SOFC. In order to extend our research work, the electrochemical properties of Sr doped Sm_2NiO_4 materials supported on $Ce_{0.9}Gd_{0.1}O_{1.95}$ (CGO) based electrolyte and the kinetics of oxygen reduction on these electrodes are studied.

2. Experimental

The single-phase $Sm_{2-x}Sr_xNiO_4$ ($0.5 \le x \le 1.0$) powders were prepared using the glycine-nitrate process (GNP) [15]. The obtained materials were denoted, for example, as SSN1505 for $Sm_{1.5}Sr_{0.5}NiO_4$, SSN1406 for $Sm_{1.4}Sr_{0.6}NiO_4$, and so on. The $Ce_{0.9}Gd_{0.1}O_{1.9}$ (CGO) powders were prepared according to reference [16]. CGO powders were first pressed uniaxially at 220 MPa to form a pellet and then sintered at 1400 °C for 10 h. The $Sm_{2-x}Sr_xNiO_4$ powders were mixed with ethylene glycol to form ink, which was subsequently painted on one side of the CGO pellet to form a working electrode with area of 0.3 cm^2. Platinum paste was painted on the other side of the pellet in symmetric configuration, as the counter electrode (CE). A Pt wire was used as reference electrode (RE) and put on the same side of the working electrode. The RE was normally placed 2–5 mm from the WE, ensuring that this distance was at least three times the thickness of the electrolyte. Pt gauze, attached to a Pt wire, was then press-contacted to the SSN and Pt paste electrodes with the aid of a spring-loaded ceramic cap, thus serving as the final current collector. The cell was first heated up to 500 °C to eliminate organic binders, followed by sintering at 1000 °C for 2 h in air. The structure and phase stability of the materials were characterized by X-ray powder diffraction on a (Rigaku) D/MAX-3B diffractometer (Cu Kα radiation). The morphology and microstructure of the sintered electrodes were examined with Hitachi S-4700 FEG-SEM. The impedance spectra were recorded over the frequency range 1 MHz to 0.1 Hz using Autolab PGStat30. The measurements were performed at equilibrium potential as a function of temperature (500–700 °C) and oxygen partial pressure (in an N_2/O_2 mixed atmosphere). The dc polarization experiments were performed by the chronoamperometry method [17], which involved a potential step followed by recording the current density as a function of time. The cathode overpotential was calculated according to the following equation.

$$\eta_{WE} = \Delta U_{WR} - iR_{el}$$

where η_{WE} represents the cathode overpotential, ΔU_{WR} the applied voltage between working electrode and reference electrode, i the current flowing through the test cell and R_{el} is the resistance of the electrolyte obtained from the impedance spectrum.

3. Results and discussions

3.1. Chemical stability of the cathode material

Fig. 1(a) was the XRD pattern of prepared $SmSrNiO_4$ (SSN1010) powders. It was observed that SSN1010 crystallized in a single phase with K_2NiF_4-type structure, no impurities

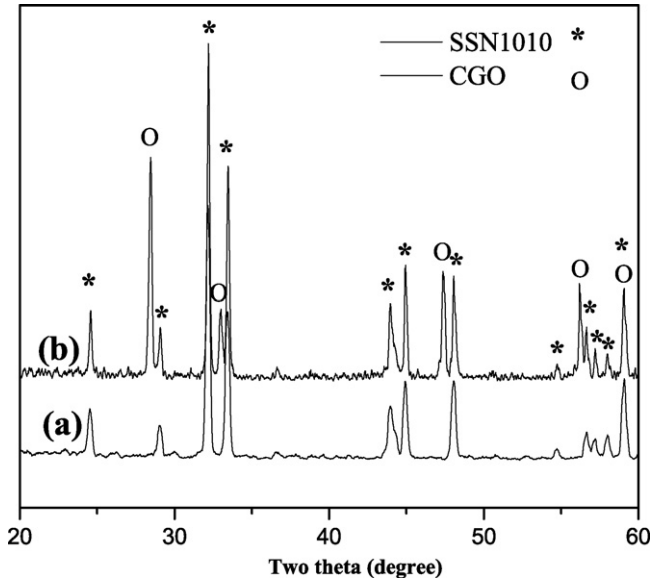

Fig. 1. XRD patterns of SSN1010 (a) and SSN1010-CGO mixtures (b) after heated at 1100 °C for 2 h in air.

were found. As we know, the reaction between electrode and electrolyte is undesirable for long term stability of SOFC. The reactivity of SSN1010 with CGO electrolyte was further studied by mixing thoroughly SSN1010 with CGO powders in a 1:1 weigh ratio, and then sintered at 1100 °C for 2 h. Clearly, there were no new peaks identifiable or shift of XRD peaks in the pattern (Fig. 1(b)), indicating that there was no reaction and/or inter-diffusion of elements occurred between SSN1010 and CGO. This result revealed that SSN1010 had good chemical compatibility with the CGO electrolyte.

3.2. Electrochemical measurements of the cathode material

In order to investigate the effect of sintering temperature on the SSN cathode properties, a number of different sintering conditions were studied. Fig. 2 is the impedance spectrum of the cathode sintered at different temperatures for 2 h and then measured at 700 °C in air. The intercepts of the impedance arcs with the real axis at high frequencies correspond to the resistance of the electrolyte and lead wires, while the overall size of the arcs is attributed to cathode polarization resistance (R_p). From the impedance spectrum, we observed that R_p was relatively large when the sintering temperature was low (900 °C). When the sintering temperature was 1000 °C, R_p reduced to the lowest value. R_p increased again when the sintering temperature was up to 1100 °C. As we know, the sintering temperature has a dramatic effect on the electrode microstructure, which in turn will influence the electrode properties. Therefore, the microstructural evolution of the SSN cathode at different sintering temperatures was further studied. Fig. 3 is the typical SEM image of the SSN electrode after sintering at different temperatures for 2 h. It was observed that SSN particles formed poor contacts with each other when the sintering temperature was 900 °C (Fig. 3(a)). Sintering at 1000 °C resulted in a structure with moderate porosity, and strong contact between the SSN electrode and the CGO

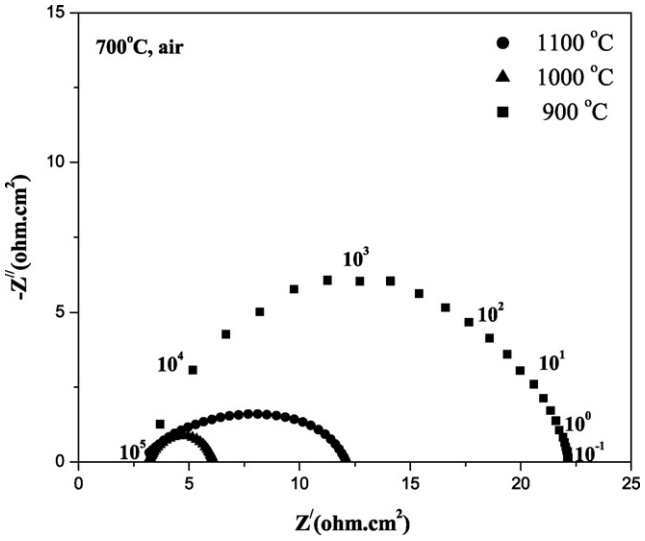

Fig. 2. Impedance spectrum of the SSN1010 cathode sintering at different temperatures for 2 h and then measured at 700 °C in air.

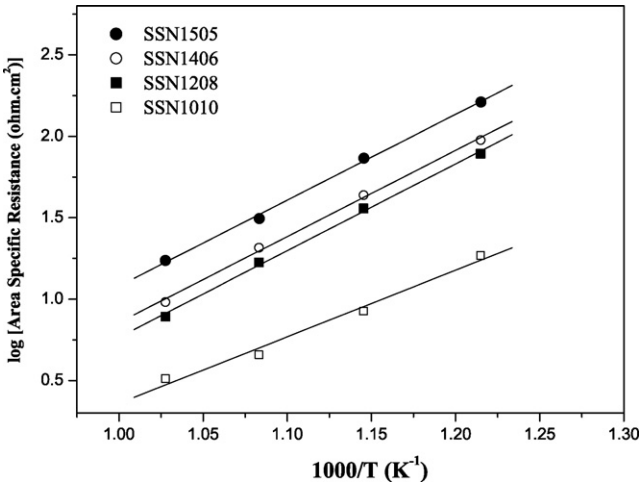

Fig. 4. Arrhenius plots of the area specific resistance of SSN electrodes measured in air.

electrolyte. The average particle size was about 1.5 μm, and the thickness of the electrode was about 25 μm (Fig. 3(b and d)). When the electrode was sintered at 1100 °C for 2 h, however, an over-sintering phenomenon was observed (Fig. 3(c)). This effect decreased the electrode porosity and triple phase boundary (TPB) length, resulting in a increase of R_p. A similar effect has been observed before in the literature [18]. Hereafter, the studied electrode was sintered at 1000 °C for 2 h to obtain the best sintering performance.

The temperature dependence of polarization resistance for $Sm_{2-x}Sr_xNiO_4$ ($x = 0.5, 0.6, 0.8, 1.0$) materials is given in Fig. 4. The polarization resistance decreased with the increase of the Sr-doping content over the entire examined temperature range. This may be attributed to the loss of lattice oxygen and the formation of oxygen vacancies, a process enhanced by the Sr-doping [19]. The area specific resistance (ASR) of $Sm_{1.0}Sr_{1.0}NiO_4$ at

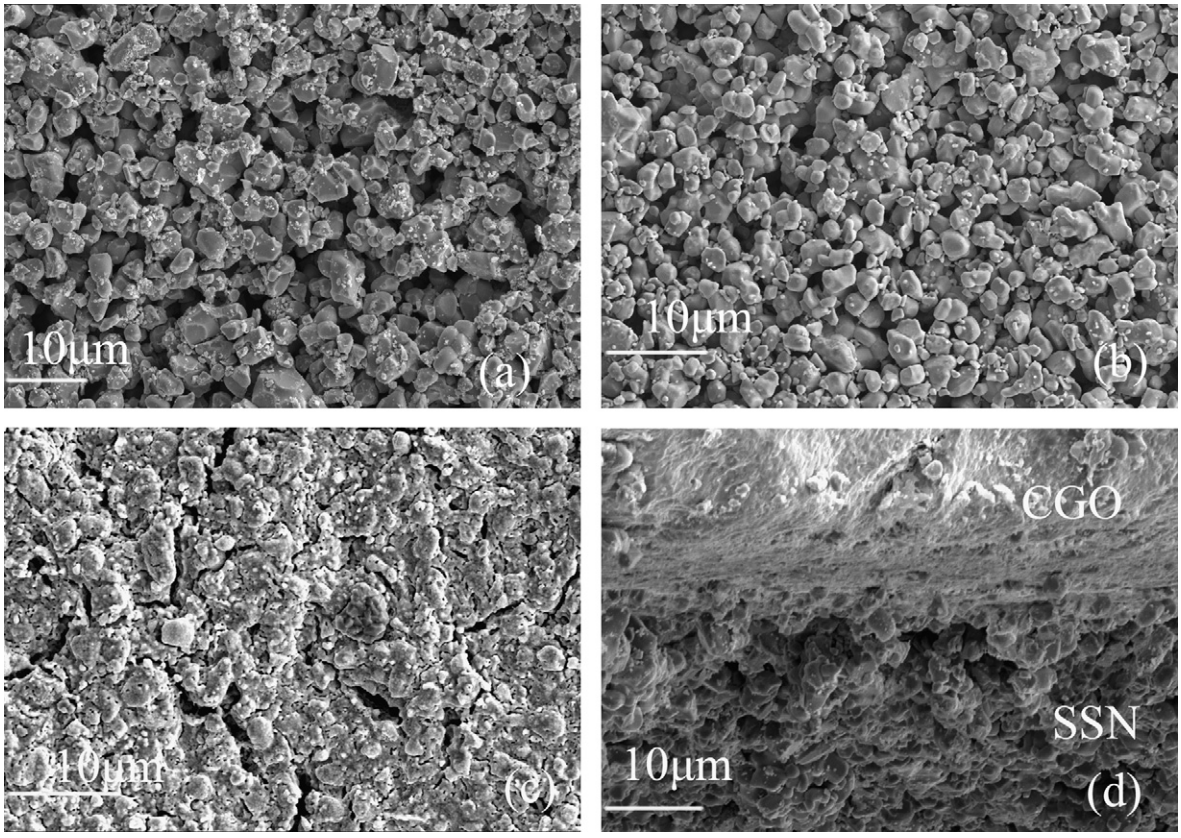

Fig. 3. SEM images of the SSN electrode sintered at 900 °C (a); 1000 °C (b); 1100 °C; (c) the cross-section image of the test cell (d).

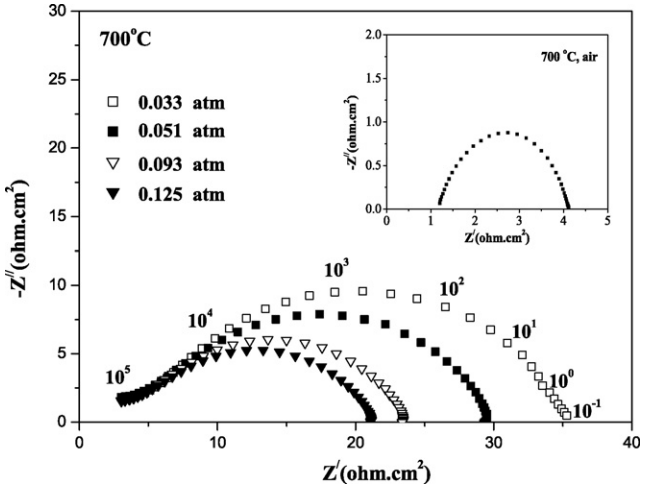

Fig. 5. Impedance spectra for the SSN1010 cathode measured at 700 °C under various oxygen partial pressures.

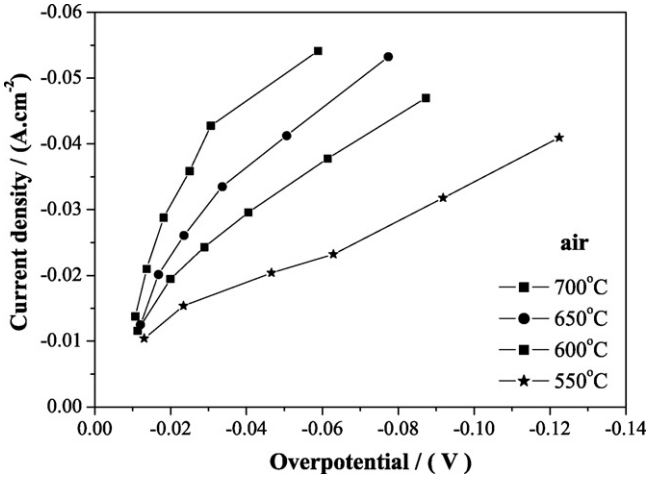

Fig. 7. Cathodic overpotential for SSN1010 at different temperatures as a function of current density.

700 °C was about 3.06 Ω cm^2 in air, similar to that of the reported $La_{1.6}Sr_{0.4}NiO_4$ and $SmSrCoO_4$ electrode material [12,13], but still is higher than well-known materials, such as LSCF.

Fig. 5 is a typical impedance spectrum of the test cell measured at 700 °C under different oxygen partial pressures (P_{O_2}). The polarization resistance (R_p) decreased dramatically with the increase of P_{O_2}. Generally, R_p varies with the oxygen partial pressure according to the following equation:

$$R_p = R_p^0 (P_{O_2})^n$$

The value of n could give useful information about the type of species involved in the reactions [20,21]:

$n = 1$, $O_2(g) \Leftrightarrow O_{2,ads.}$

$n = \frac{1}{2}$, $O_{2,ads.} \Leftrightarrow 2O_{ads.}$

$n = \frac{1}{4}$, $O_{ads.} + 2e' + V_O^{\bullet\bullet} \Leftrightarrow O_O^x$

The dependence of polarization resistance on oxygen partial pressure was shown in Fig. 6. The linear variation of R_p with oxygen partial pressure indicates that at a given temperature, the rate limiting step does not significantly depend on the oxygen composition of SSN1010. However, from the calculated n values shown in Fig. 6, the reaction rate limiting step clearly depends on the temperature. With temperature increasing from 600 to 700 °C, the reaction rate limiting step would be a process involving successively the incorporation of oxygen into the oxide lattice and the dissociation of molecular oxygen. A similar result has been reported before in the investigation of a Nd_2NiO_4 cathode [22].

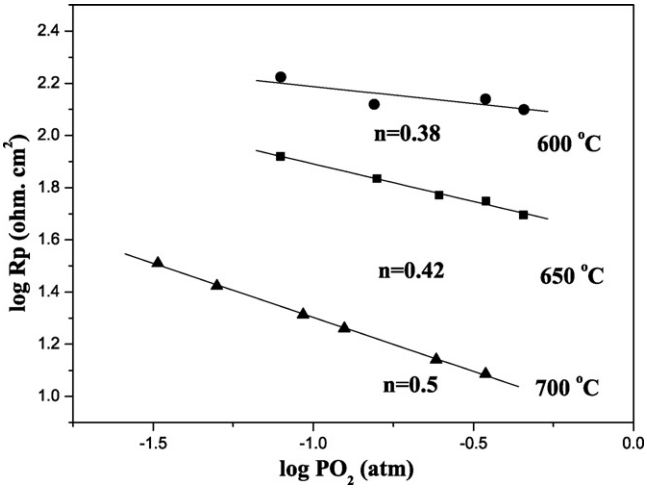

Fig. 6. R_p of SSN1010 vs. oxygen partial pressures at various temperatures.

Cathodic overpotential is an important parameter for SOFC. The cathodic overpotential as a function of current density at different temperatures is plotted in Fig. 7. At low overpotentials (less than 20 mV), we can expect a linear expression [23], $i = i_0 ZF\eta/RT$, where i is the current density, i_0 the exchange current density, n the overpotential, F is the Faraday's constant, and R is the universal gas constant. From the inverse of the derivative of i against n, we can obtain the area specific resistance. The value obtained at 700 °C in air was 2.91 Ω cm^2, which was in agreement with the result obtained from impedance measurement. It is observed from Fig. 7, that the current density increases with increasing temperatures. The lowest polarization overpotential, 58.9 mV was measured for SSN1010 cathode at a current density of 54.1 mA cm^{-2} at 700 °C in air. This value is similar to that of the reported $La_{2-x}Sr_xNiO_4$ materials in literature [12]. As we expected, the high electrical conductivity combined with large amount of oxygen vacancy formed by Sr-doping in SSN materials makes low polarization possible. Compared to the LSCF material, the polarization resistance of SSN cathode is quite high. Whereas considering the thermal expansion coefficient (TEC), $Sm_{2-x}Sr_xNiO_4$ has a much similar TEC ($Sm_{1.4}Sr_{0.6}NiO_4$, 11.8×10^6 K^{-1} in air [14]) compared to that of the CGO electrolyte, and the TEC value of LSCF material is quite large ($La_{0.6}Sr_{0.4}Co_{0.2}Fe_{0.8}O_4$: 17.5×10^6 K^{-1} in air [6]). Therefore, the SSN material can be considered as a promising cathode candidate for the IT-SOFC, given that the electrode performance can be further improved by optimizing the microstructures and/or forming composite cathodes.

4. Conclusions

1. The SSN cathode forms good contact with the CGO electrolyte after sintering at 1000 °C for 2 h.
2. The reaction rate limiting step on the cathode depends on the temperature.
3. The area specific resistance obtained at 700 °C in air is about 3.06 $\Omega\,cm^2$ for the SSN1010 electrode, and the lowest overpotential is 58.9 mV at a current density of 54.1 $mA\,cm^{-2}$.

Acknowledgements

The Project was supported by Science Foundation for Distinguished Young Scholars of Heilongjiang Province and Key Project of Chinese Ministry of Education (206044, 205050).

References

[1] S.B. Adler, Chem. Rev. 104 (2004) 4791–4844.
[2] S. Charojrochkul, K.L. Choy, B.C.H. Steele, Solid State Ionics 121 (1999) 107–113.
[3] N.T. Hart, N.P. Brandon, M.J. Day, N. Lapena-Rey, J. Power Sources 106 (2002) 42–50.
[4] S.C. Chen, K.V. Ramanujachary, M. Greenblatt, J. Solid State Chem. 105 (1993) 444–457.
[5] V.V. Vashook, I.I. Yushkevich, L.V. Kokhanovsky, L.V. Makhnach, S.P. Tolochko, I.F. Kononyuk, H. Ullmann, H. Altenburg, Solid State Ionics 119 (1999) 23–30.
[6] M.A. Daroukh, V.V. Vashook, H. Ullmann, F. Tietzb, I. Arual Raj, Solid State Ionics 158 (2003) 141–150.
[7] S.J. Skinner, J.A. Kilner, Solid State Ionics 135 (2000) 709–712.
[8] E. Boehm, J.M. Bassat, P. Dordor, F. Mauvy, J.C. Grenier, Ph. Stevens, Solid State Ionics 176 (2005) 2717–2725.
[9] J.A. Kilner, C.K.M. Shaw, Solid State Ionics 154 (2002) 523–527.
[10] V.V. Vashook, S.P. Tolochko, I.I. Yushkevich, L.V. Makhnach, I.F. Kononyuk, H. Altenburg, J. Hauck, H. Ullrnann, Solid State Ionics 110 (1998) 245–253.
[11] K. Ishikawa, S. Kondo, H. Okanc, S. Suzuki, Y. Suzuki, Bull. Chem. Soc. Jpn. 60 (1987) 1295–1298.
[12] Q. Li, Y. Fan, H. Zhao, L.H. Huo, Chin. J. Inorg. Chem. 22 (2006) 2025–2030.
[13] Y.S. Wang, H.W. Nie, S.R. Wang, T.L. Wen, U. Guth, V. Valshook, Mater. Lett. 60 (2006) 1174–1178.
[14] H.W. Nie, T.L. Wen, S.R. Wang, Y.S. Wang, U. Guth, V. Vashook, Solid State Ionics 177 (2006) 1929–1932.
[15] L.A. Chick, L.R. Pederson, G.D. Maupin, J.L. Bates, L.E. Thomas, G.J. Exarhos, Mater. Lett. 10 (1990) 6–12.
[16] C. Xia, W. Rauch, F. Chen, M.L. Liu, Solid State Ionics 149 (2002) 11–19.
[17] A. Espuirol, N. Brandon, N. Bonanos, J. Kilner, M. Mogensen, B.C.H. Steele, in: A.J. Mc Evoy (Ed.), Proceedings of the Fifth European Solid Oxide Fuel Cell Forum, U. Bossel, Oberrohrdorf, Switzerland (publ.), 2002, p. 225.
[18] H. Zhao, L.H. Huo, L.P. Sun, L.J. Yu, S. Gao, J.G. Zhao, Mater. Chem. Phys. 88 (2004) 160–166.
[19] L.W. Tai, M.M. Nasrallah, H.U. Anderson, D.M. Sparlin, S.R. Sehlin, Solid State Ionics 76 (1995) 259–271.
[20] Y. Takeda, R. Kanno, M. Noda, O. Yamamoto, J. Electrochem. Soc. 134 (1987) 2656–2661.
[21] E. Sicbeit, A. Hammouche, M. Kleitz, Electrochim. Acta 40 (1995) 1741–1753.
[22] F. Mauvy, J.M. Bassat, E. Boehm, J.P. Manaud, P. Dordor, J.C. Grenier, Solid State Ionics 158 (2003) 17.
[23] B.C.H. Steele, Solid State Ionics 75 (1995) 157–165.